Jerzy MERKISZ,
Marek WALIGÓRSKI

PTNSS–2011–SC–129

The application of the deterministic chaos method in the assessment of the combustion process in diesel engines fitted in non-road vehicles

Abstract: The paper describes the problem of the combustion process diagnostics in diesel engines of HDV vehicles in the aspect of the environment protection and misfire detection as well as its use in the OBD/EOBD systems. Vibroacoustic processes were taken into consideration and the chosen parameters of the vibration signals obtained from the specified locations in the engine were the diagnostic estimators of the process changes. The paper discusses the diagnosis of the course of the process from the point of view of the OBD system requirements, in order to check the possibility of using the deterministic chaos method and vibroacoustic processes in on-line diagnostic processes and in the design of combustion monitors in diesel locomotive engines. This stage of the scientific studies was done to check the sensitivity of selected non-linear methods for the process changes or their lack. The paper also presents the signal analyses, limitations of the method, criteria of the process qualification and its accuracy. Diagnostic algorithms of misfire detection and possibility of its practical use in contemporary vehicle drivertrains have been described as well.

Key words: *combustion process, misfire, diagnostics, vibroacoustics, environment protection, OBD system, and deterministic chaos theory*

Zastosowanie metody chaosu deterministycznego w ocenie poprawności procesu spalania w silnikach ZS pojazdów pozadrogowych

Streszczenie: W pracy opisano problematykę diagnostyki procesu spalania dla silników ZS pojazdów typu HDV (Heavy-Duty Vehicles) w aspekcie ochrony środowiska naturalnego i wykrycia braku zapłonu oraz jej zastosowania w systemach OBD/EOBD. W pracy rozważano procesy wibroakustyczne, wybrane parametry sygnałów drgań uzyskanych z określonych miejsc na silniku stanowiły estymatory diagnostyczne zmian procesu. Artykuł dotyczy diagnozy przebiegu procesu z punktu widzenia wymagań diagnostyki OBD i takiegoż systemu, dokonano sprawdzenia możliwości zastosowania metody chaosu deterministycznego i procesów wibroakustycznych do bieżącej diagnostyki spalania i budowy monitora diagnostycznego w silnikach lokomotyw spalinowych. Powyższy etap badań naukowych był zrealizowany w celu kontroli wrażliwości wybranych metod nieliniowych na zmiany procesu lub jego brak. Przestawiono również analizy sygnałów i ograniczenia zastosowania metody oraz możliwości jej praktycznego zastosowania w obecnych źródłach napędu pojazdów.

Słowa kluczowe: *proces spalania, wypadanie zapłonu, diagnostyka, wibroakustyka, ochrona środowiska naturalnego, system OBD, teoria chaosu deterministycznego*

1. Non-linearity of internal combustion engines

The signals obtained from the measurements compose one-dimensional time series. The time series are processed using such methods as spectral analysis and nonlinear analysis that are based on the deterministic chaos theory. The deterministic chaos theory is a description of nonlinear dynamic systems. So far, for the improvement of the monitoring, diagnostic and control of technical devices linear methods have been used. Some elements of nonlinearity were introduced but not directly in classic linear approach [20]. The deterministic chaos theory is quite good for such analyses because it uses direct nonlinear models. The deterministic chaos theory is a continuation of the classic theory of linear dynamic systems [3, 22]. The deterministic chaos can be described as 'unpredictable long time behavior of deterministic dynamic system which is caused by the sensitivity on an initial condition'.

We must stress that nonlinear chaotic system is a fully deterministic system and it is fully predictable if we have full knowledge about the initial conditions. The chaotic system is very sensitive to even very small changes in the initial conditions, hence in most of the practical cases, where the initial conditions are known only with a given accuracy, it is really unpredictable. The nonlinear chaotic system can produce a signal that is irregular and seems similar to a stochastic system but its irregularity has a non-stochastic nature, and is caused by the internal nonlinearity of the

dynamics. Changing the values of the parameters of a nonlinear chaotic system we can find qualitative changes of the solution, which is particularly well seen in the phase space.

Many processes in the technical area, describing electric and mechanical devices, contain nonlinear elements in their dynamics [13, 14, 18]. This can be used to improve the monitoring, diagnostic and control of technical devices. In literature we can find a term 'engineering chaos' for a description of the deterministic chaos theory application for engineering and industrial purposes [13]. The combustion engines can be a source of many signals which are good for analysis – it is enough to mention the vibration signals from sensors fitted in the engine, all acoustic signals, signals from the ionic current detectors, signals representing crankshaft angular velocity, pressure signals, and even visual signals that can for example show the engine head heating [27]. The combustion engine shows a cyclic variability of energy release from one cycle to another. In literature the cyclic variability is described in a stochastic, linear deterministic or chaotic deterministic way, and all the time we can find the discourse on the real nature of the cyclic variability [9–11, 19, 24]. The nonlinear methods started to play an important role in engine dynamic modeling. This approach can allow us a better understanding of the dynamics of engine processes [9–12, 17, 18, 26].

Suppose that there is the sampled time signal s(t). The main idea of the approach presented in the paper is as follows: the space in which we should observe the dynamic signal structure is not one-dimensional space of s(t) values but a higher-dimensional dynamic space of some original vectors y(t). Hence, the main task is to find the right dimension of the original phase space and the dynamic parameters characterizing the dynamic evolution. What we can really do is to identify the space, which is formally equivalent to the original phase space. This can be done by applying the Takens and Mañé theorem [1, 15]. The main problems are to find the time-delay value and the dimension. The way to accomplish this purpose is to apply time-delay embedding and false nearest neighbor method. The time delay is usually found as the first zero of the autocorrelation function or as the first minimum of averaged mutual information [1, 15]. Having the time interval τ we use its increasing multiples as: $s(t)$, $s(t+\tau)$, $s(t+2\tau)$, $s(t+3\tau)$...

If it is considered the time series $s(n)$ with t_p sample time, then $s[n] = s(nt_p)$ and the sequence of delay vector components started from time t_i can be written as:

$$s[i] = s(t_i), \tag{1}$$

$$s[i + T] = s(t_i + \tau), \tag{2}$$

$$s[i + 2T] = s(t_i + 2\tau)... \tag{3}$$

where $T = t/t_p$. Starting with t_1 the successive points in n-dimensional-phase space created from n delay components can be written as:

$$y(1) = (s[1],s[1 + T],s[1 + 2T],...,s[1 + nT]) \tag{4}$$

$$y(2) = (s[2],s[2 + T],s[2 + 2T],...,s[2 + nT]) \tag{5}$$

$$y(3) = (s[j],s[j + T],s[j + 2T],...,s[j + nT]) \tag{6}$$

To find the right dimension we can apply the false nearest neighbor method. The method includes the successive growth of the dimension and the selection of the right dimension for a given process is realized in such a way that the geometrical structure formed in the subsequent phase spaces is fully developed (in the geometrical sense and in the sense of the determined structure features). This means that the near distance of all points is the result of only the dynamics, not of the projection into space of lower dimension. The algorithm for all vectors in the phase space tests their neighbors and checks if they are false or true neighbors. As the right dimension, we chose the one for which the percentage of false neighbors (which are the result of a projection) decreases to zero. The time-delay value and the dimension are parameters that can also be useful from the diagnostic point of view. But, for a diagnostic purpose, it is better to use the parameters describing the dynamics in the phase space. The presented investigations used the Lyapunov exponents, especially the dominant Lyapunov exponent. The Lyapunov exponents represent an average convergence (or divergence) speed of two neighbor trajectories. One has a convergence for $\lambda > 0$ and divergence for $\lambda < 0$. In a non-linear system with d degrees of freedom (d-dimensional phase space) one has d Lyapunov exponents $\lambda_1 > \lambda_2,...,\lambda_\delta$. Usually, if one of the Lyapunov exponents is positive, we can expect a chaotic behavior. Analysis of Lyapunov exponents can give information about bigger or smaller chaotic contribution in the system. Anyway, the Lyapunov exponents can be treated as parameters that can be directly applied during the diagnostic process to differentiate one system state from another [1, 15].

In the approach for finding the right dimension the false nearest neighbor method can be used. The method is performed as follows [1, 16]. Consider the vectors in d-dimensional reconstructed space. For each d-dimensional vector $x_d=(x_1, x_2,...,x_d)$, we try to find the nearest d-dimensional neighbor $y_d=(y_1, y_2, y_3,...,y_d)$ and the distance $\|x_d-y_d\|$. If the vector y_d is a true neighbor of x_d, then it should be contained in the neighborhood of x_d during all the dynamic evolution. If y_d is a false neighbor of x_d

then going into a higher dimension d+1 it can shift outside the x_d neighborhood. It is needed the criterion is found if x_d and its neighbor y_d from d-dimensional space are neighbors in the (d+1)-dimensional space. To do this we go into dimension d+1 and calculate:

$$R_d = \frac{\|x_{d+1} - y_{d+1}\|}{x_d - y_d} \tag{7}$$

The main criterion here is as follows: if R_d exceeds threshold value pr_1:

$$R_d > pr_1 \qquad \frac{\|x_{d+1} - y_{d+1}\|}{x_d - y_d} > pr_1 \tag{8}$$

The vector y is treated as a false neighbor. It can be signed:

$$D(d) = (x_1 - y_1)^2 + (x_2 - y_2)^2 + \ldots + (x_d - y_d)^2 \tag{9}$$

then it is $D(d+1)=D(d)+(x_{d+1} - y_{d+1})^2$. Now the criterion (8) can be written as:

$$\frac{\|x_{d+1} - y_{d+1}\|}{x_d - y_d} = \frac{\sqrt{D(d+1)}}{D(d)} > pr_1 \tag{10}$$

Eventually, the criterion (8) can be written as:

$$\frac{|x_{d+1} - y_{d+1}|}{\sqrt{D(d)}} > pr_1 \tag{11}$$

The problem appears because $D(d)$ is greater for higher dimensions [1, 16]. It is expected that the threshold value should also increase together with the dimension. Eventually, one uses the criterion (9) in the form:

$$\frac{|x_{d+1} - y_{d+1}|}{\sqrt{D(d)}} > \frac{pr_1}{\sqrt{d+1}} \tag{12}$$

where the term $\sqrt{d+1}$ performs the correction of the D(d) increase.

In literature we can find more criteria, but all of them consider the properties of the attractor. In a situation when one knows nothing about the dynamic structure of the problem such criteria are worthless. Hence, in a general situation when there is no information about the attractor structure the only good approach is to use criterion (12) or (8). The experiments from [23] present the tendency that the percentage of false nearest neighbors shows the stable value in the values range of ($10 \le R_p \ge 30$). The recommended threshold value in literature is R_p = 17.3. In the experiments one calculated the dependence of dimension d on the threshold value T. It is interesting that most of our experiments (fig. 1) show the short but very well-signed plateau, where the dimension is independent of the threshold value. There is the confirmation of the suggestions of Rhodes [23].

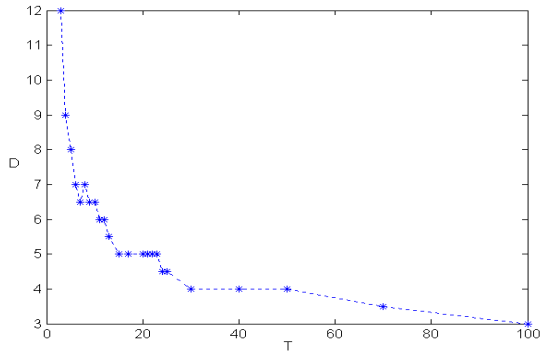

Fig. 1. The exemplary plot of dependence of dimension D on threshold value T for the given signal in false nearest neighbor method

The eventual algorithm that the authors proposed is as follows: for each signal (time series) after finding the time delay τ, one should perform the experiments for finding dependency d on threshold value T. For the right dimension we should take the value corresponding to the plateau (for the plot in fig. 1 it will be value d = 3 and T = 40). It is noteworthy that our results show that we cannot use one threshold value for all signals. For different signals we very often find different ranges of plateau. In our experiments for the same type of signals the plateaus were nearly the same, but for different signals obtained from different sources they differed [2, 16, 23].

2. Methodology, test stand and measurement conditions

The authors performed a specified investigation of misfire detection from the point of view of the on-line diagnosis of the combustion process and its absence. The paper considers the phase of the investigations that were conducted in potential operating conditions on a 2112 SSF (SU45 diesel locomotive) and 16H12A engine (401Da diesel locomotive) – table 1.

The measurement signals obtained from the transducers were fed to the amplifiers where they were amplified and normalized. They were subsequently fed to the analog inputs of the data acquisition card. Measurement signals were filtered inside the card with the help of analog and digital filters and then were converted from analog to digital. The signals obtained in the data acquisition card in a digital form were stored in a computer memory. The recorded all time history courses of

the measurement signals were subjected to the time selection process. In the above selection all recorded signals were divided into signal sequences including single working cycles of the internal combustion engine.

Table 1

The features of the engines used in the investigations

Feature/parameter	Type of engine	
	2112 SSF	16H12A
Type	CI, 4-stroke	CI, 4-stroke
Cylinder bore × piston stroke: $D \times S$ [m]	0.210×0.230	0.135×0.155
Compression ratio (ε)	11.3	14.0
Engine displacement (V_{ss}) in [m^3]	$96.6*10^{-3}$	$26.6*10^{-3}$
Type of injection pump	PLD system	Line injection pump
Number of valves	4	4
Injector opening pressure (p_{wtr}) in [MPa]	$26 \pm 0{,}5$	19 ± 0.5
Cylinder system/number	V12 – 90^o	V12 – 60^o
Mean effective pressure in [MPa]	1.37	0.77
Maximum effective power (N_e) in [kW]	1655 (1500 rpm)	257 (1500 rpm)

The divided measurement signals allowed the authors of the paper to consider the influence of the single combustion process on the selected vibration signal parameters and as a consequence, calculate the differences of these parameters for the proper combustion process and cycles, in which misfire events occurred.

In the investigations on the SU45 diesel locomotive engine, the selection of the operating conditions of the engine was made based on the useful rpm and torque range of the tested engine corresponding to the operating conditions. The measurements were divided into two parts. In the first of them all cylinders of one bank were taken into consideration to check if it is possible to use the vibration characteristics in the assessment of the combustion process course for an engine being used in traction vehicles. This stage was also used to see the differences in the sensibility of the vibration signal in each working cylinder. This helped to determinate the best and worst conditions for misfire detection based on the vibration methods. The second research stage was used to determine the differences between signals with combustion and misfire for different working points (power changes) for 3 cylinders taken from the previous stage. In the first stage the following engine speeds were taken into consideration: 700, 900, 1080, 1300 and 1500 rpm. The following effective power was obtained: ~ 0 (idling run), 252, 460, 580, 667 kW. In the second test stage all engine speeds and torques defined with the locomotive regulating unit position were taken as the working points. The test measuring points were located in the engine head and the signals were recorded in the Z direction (parallel to the cylinder axis forward of the piston movement). The points were selected according to the principle that the sensor should be placed closest to the point where the tested process-related vibration signal is generated.

The misfire during the tests on the 16H12A diesel locomotive engine was simulated by the disconnection of one cylinder of the engine. The acceleration sensor was fixed into the engine frame in the place, where one could define the measurement direction of acceleration. First of all, a 16-channel digital recorder TA11 was applied produced by Gould based on piezoelectric sensor 4395 produced by Brűel & Kjær. The authors also used a data acquisition program Gould Acquire TA-D and the results analysis program DASA VIEW II produced by Gould.

The measurement of the 16H12A locomotive engine was performed in the following circumstances:

1. three engine speeds
   a) n1 = 650–680 rpm (idle run),
   b) n2 = 1100 rpm,
   c) n3 = 1500 rpm,
2. three measurement phases
   a) phase 1 – sensor is fixed on cylinder 1 – all cylinders are working,
   b) phase 2 – sensor is fixed on cylinder 1 – cylinder 1 is disconnected,
   c) phase 3 – sensor is fixed on cylinder 1 – cylinder 4 is disconnected.

The sensor was fixed on the frame of cylinder 1.

The signals were recorded in three directions: parallel to the main locomotive axis, horizontal-transverse and vertical-transverse to the main

locomotive axis (second and third directions were taken only to compare signals with the Z direction). The engine head was the place where the vibration transducers were located.

3. JTFA vibration signals analysis

The analysis of the vibrations that are generated by the engine, in the range of a single engine working cycle, we can state that it is a process changing in time, both in the amplitude and frequency domains, as a result of subsequent engine work phases. The application of joined selections, such as e.g. space-spectral [5] or time-spectral [4] selections is purposeful in the engine diagnostics. The potential wide chances for development and use are seen nowadays for methods that are being developed at present and are based on time-spectral domain analysis. The most popular are: Short Time Fourier Transform (STFT), Wavelet Transform (WT) and Wigner Ville Distribution *(*WVD) [25].

STFT transform consists of the FFT analysis of short sequences of a signal that can be treated as a quasi-stationary signal. The input signal extraction of the following data segments to FFT analysis is realized with the use of the moving window technique [8]. The time-spectral map of the process analyzed is obtained when the received spectra are put together. A result the STFT analysis can be treated like a series of spectra determined for local, short time segments. The method advantages are: a short time of a time-frequency map determination, an easy and intuitive results interpretation and a constant resolution for all frequencies. The result form depends on the taken time window function and signal processing parameters: a number of samples in the data segments and the time step of the analysis. The limitation of the method is that it is impossible to obtain a high resolution for time and frequency domains at the same time. The resolution in the time domain can be improved by using an overlapping consisting in partial interference of the analyzed signal segments to each other. An estimation error of the amplitude and frequency for local maximum values on a map can be minimized by using an amplitude-frequency correction – AFC [6, 7].

The mother functions can be each function in the Wavelet transform [21]. The Morlet's function as a mother function is used in many cases because of the calculation process simplification. Its application allows using the FFT procedure in the processing, which accelerates the calculation process effectively. The result form depends mostly on the taken mother functions. This type of an analysis can be equated to a filtration with a constant relative bandwith $\Delta f/f_s$. The filter position on the time-frequency map is given by scale and translation parameters (a – dilation, b – translation). The analysis bandwidth increases along with the translation to higher frequencies (a resolution of an analysis in the frequency domain decreases). Then, the resolution in the time domain increases, and vice versa. That feature is useful in the case of a simultaneous analysis and observation with a different time step for a rapid changeable and high-frequency processes (e.g. a valves opening and closing, a combustion process) and slow-speed low-frequency processes. The drawbacks of the method are: the form of the result depends on a taken mother function and the interpretation of a graphical form of a result is not always intuitive.

Wigner-Ville distribution (WVD) is realized by two-dimensional time-frequency window. This kind of an analysis allows taking any size of an analysis window theoretically. When an analysis window size is defined arbitrarily, it may give negative distribution values, arising interferences in the time and frequency domains, which makes the interpretation process more difficult. The WVD distribution characterizes a long time of the calculations, especially for long time series, comparing to the previous methods.

The combinations of different methods of a signal selection (e.g. time and amplitude selection), apart from the basic methods of a vibration analysis, were used during the research. The dynamics of diagnostic symptoms describing misfires increased.

The task of time-spectral selection procedures is to get out from the vibration process and/or display pieces of information connected with the combustion process in an engine cylinder. Apart from vibration transducers, the tachometric transducer was used in the phenomenon area to identify the cycle phases during the engine work. In order to decrease the estimation errors of amplitude and frequency components for map $a(t, f)$, the amplitude-frequency correction procedures can be used as an option. Further signal parameterization (creation of estimators and characteristics) should lead up to obtain symptoms that detect misfire events in an engine cylinder.

The application of a time-spectral map parameterization is necessary to obtain a complete representation of a lack of ignition in a cylinder on the based on point measures of a vibration signal. The second measurement stage was conducted on a 2112 SSF diesel locomotive engine (in regular operation). The time-spectral maps were obtained, both for a lack of combustion in a cylinder (fig. 2) and when combustion took place (fig. 3). In this case, a peak value of vibration accelerations in the range of frequency of 3000–5000 Hz, determined based of time-spectral map, was the parameter that described a lack of ignition in the cylinder or a combustion process for a diesel locomotive engine.

Parameter changes were described with the dynamics of 34 dB.

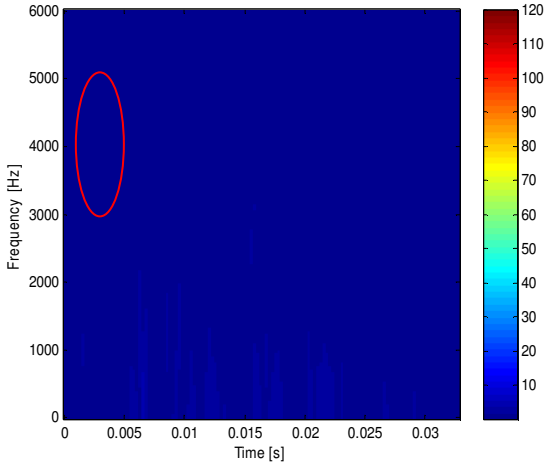

Fig. 2. The example vibration acceleration courses in the Z dimension (a_z) of cylinder heads for the 2112 SSF diesel locomotive engine (n = 700 rpm and M_o = 0 N·m) and for lack of combustion

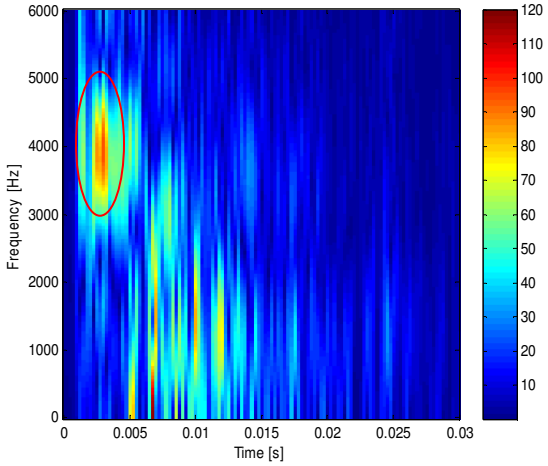

Fig.3. The example vibration acceleration courses in the Z dimension (a_z) of cylinder heads for the 2112 SSF diesel locomotive engine (n = 700 rpm and M_o = 0 N·m) and for a combustion process

4. Non-linear diagnostics of engine combustion through a vibration signal

Choice of time delay and embedding dimension

Time delay t was calculated both as the first zero cross of autocorrelation function (COR) and first minimum of averaged mutual information (AMI). The eventual value of t was usually taken from AMI because it represents real non-linear properties (fig. 4). Eventually, the decision as to which value must be selected resulted from the necessity of using the same (or similar) values of parameters for compared signals. In turn, dimension d was obtained using the method. During the analysis and finding the embedding dimension d, we took into account the dependence of the false neighbor percentage on dimension d and considered the two cases at the beginning: while the plot decreases till value 5%, while the plot decreases till value 0%. It appeared that the second case (0%) was very difficult to estimate. The decrease of the plot till real 0% was not strict and well marked, and the calculations usually were very time-consuming. The level 5% was enough because this usually indicated the area where the plot reached the plateau.

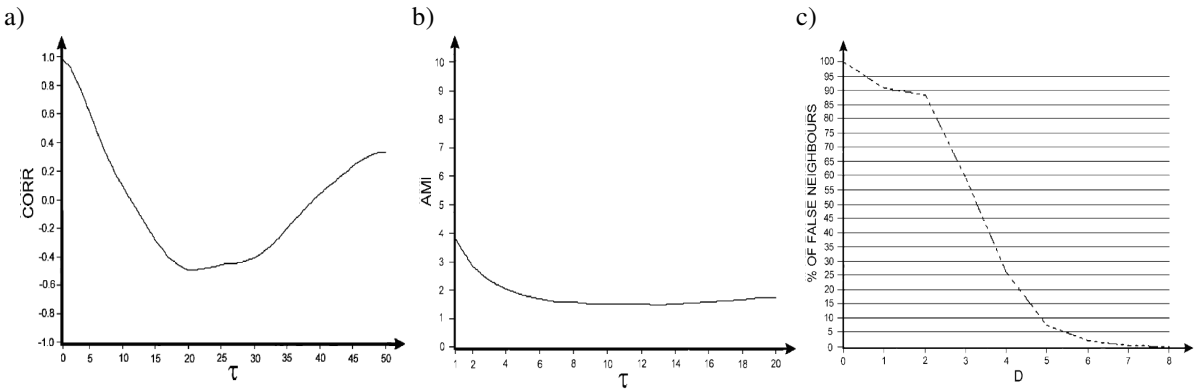

Fig. 4. Exemplary plot of autocorrelation function (a), averaged mutual information (b) and dependence of false neighbor percentage on dimension D for the 16H12A engine (n = 1500 rpm, Z direction, all cylinder work)

For the obtained signals, the time-delay value was in the range t = 12–14 (where $t_{śr}$ = 12.78), and the embedding dimension d = 5–6 (where $d_{śr}$ = 5.5). The obtained values of t and d allow observing the

time evolution in the phase space. Most of the observed geometrical objects have the form of spheres, but many of them show some subtle structures (fig. 5–7). The vibroacoustic signals were preprocessed with the use of the band filters FIR and IIR (Butterworth) a constant component is cut off, and the dominant frequency band is the same for all signals. The IIR filters for our signals appeared unstable and during the filter designing there was no influence on the phase characteristic. Eventually, the FIR filters could be used, which are better from the stability point of view and have a linear phase characteristic.

a) b)

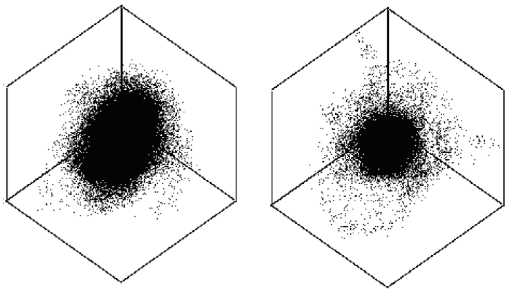

Fig. 5. The phase portrait in a three-dimensional-phase space, which is the projection from the multidimensional space: a – for the pure (without filtration) signal (n = 650 rpm), cylinder 4 does not work, direction X (τ = 12 and d = 6) and b – for the same signal after filtration (τ = 5 and d = 6)

a) b)

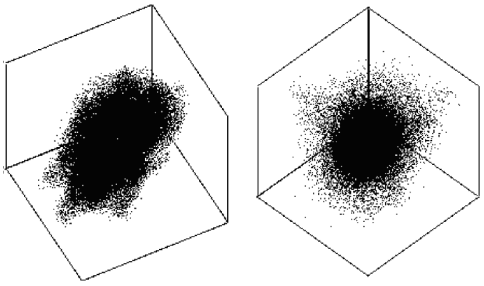

Fig. 6. The phase portrait in a three-dimensional-phase space, which is the projection from the multidimensional space: a – for the pure (without filtration) signal (n = 1100 rpm), all cylinders work, direction Y (τ = 13 and d = 5) and b – for the same signal after filtration (τ = 4 and d = 6)

The main disadvantage of FIR filter is the necessity of using high order methods, which appeared very time consuming. This unfortunately makes them impossible to use in on-line processing. In practice, we can consider the use of IIR Butterworth filters with zero phase which can be obtained by applying the filter twice, forward and backward [20]. The filtering was performed using the MATLAB software with a signal-processing toolbox. The filtrating results appear especially interesting for the calculated Lyapunov exponents. The filtering decreased the values of the time delay and also the embedding dimension. In time evolution plots we can also see some small differences. The process of filtering always gives some questions and doubts. Both the observation of the signal plot and the view of the time evolution in the phase space show that our signals are very noisy. This is always a problem how to denoise signal. Usually, a filtering leads to a loss of some signal components and we never know whether we have eliminated some important and relevant components.

a) b)

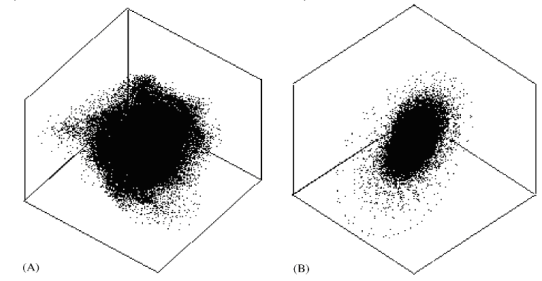

Fig. 7. The phase portrait ın a three-dimensional-phase space, which is the projection from the multidimensional space: a – for the pure (without filtration) signal 1500 rpm, all cylinders work, direction Z (τ = 13 and d = 5) and b – for the same signal after filtration (τ = 9 and d = 6)

Fig. 8 presents the fragments of engine signal plots and corresponding second line of a STFT spectrum plots. The important differences between the centers for signals with combustion and for cylinder with misfires are presented in the table 2 and the dominant Lyapunov exponents are shown in the table 3.

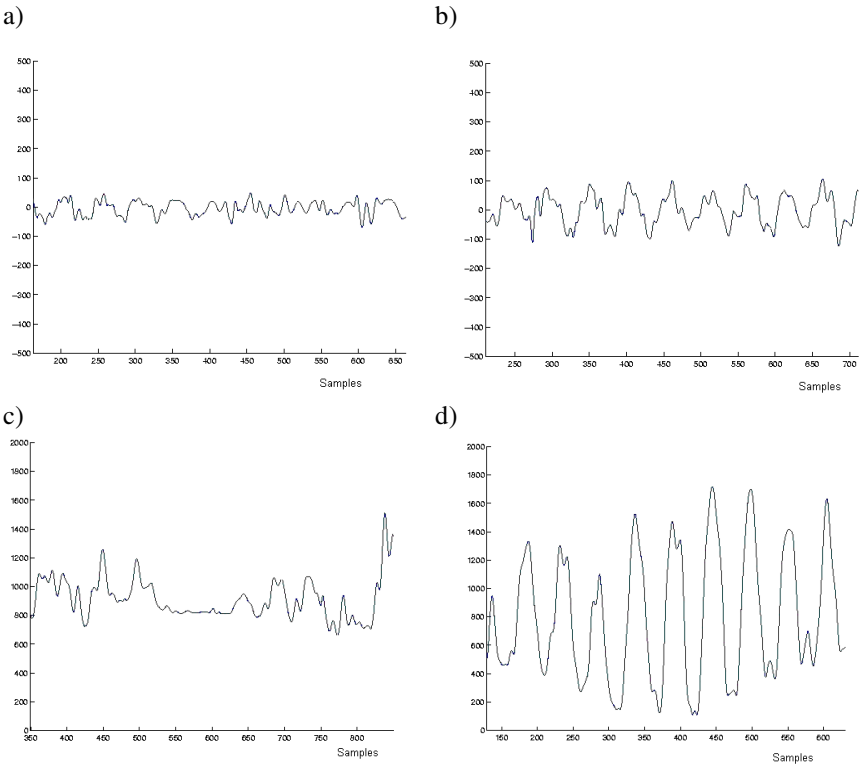

Fig. 8. Examples of plots of signals for 1500 rpm and all cylinders working (a), for 1 cylinder misfiring (b) and plots of their STFT spectrum (c) and (d) in the 2000 samples window correspondingly

Table 2

The mean coordinates of centers of 7-dimensional parameter space for signals with combustions and with misfire events for the 16H12A engine

	Window	1	2	3	4	5	6	7
		Fourier 2	Fourier 3	Fourier 4	Fourier 5	Fourier 6	Mean	Variance
All cylinders operative	0.1 s	628.93	526.62	550.79	660.96	513.13	3.50	365.10
	0.01 s	428.42	652.82	1366.78	2854.60	1156.40	0.37	7.23
Cylinder 1 misfiring	0.1 s	552.87	537.14	819.78	703.86	460.463	-0.78	233.26
	0.01 s	542.48	869.75	1656.60	3487.70	1876.68	-0.08	69.00

Table 3

The results of the dominant Lyapunov exponents calculation for the case with all cylinder working and with one cylinder disconnected

Engine speed in [rpm] and sensor number	**Dominant Lyapunov exponent**		
	All cylinders working	One cylinder disconnected	Difference
1500 1	0.573	0.519	0.054
1500 2	0.292	0.197	0.095
1500 3	0.524	0.500	0.024
1100 1	0.581	0.542	0.039
1100 2	0.355	0.327	0.028
1100 3	0.417	0.501	-0.084
650 1	0.456	0.385	0.071
650 2	0.262	0.299	-0.037
650 3	0.508	0.434	0.074

5. Conclusions

The research conducted on the diesel locomotive engines with the use of JTFA method allowed stating that:

- the method allows assessing a lack of ignition, both for a single cylinder research engine and multi-cylinder engine of a diesel locomotive,
- the time, process and frequency domain analyses ought to be used for misfire diagnosis,
- the dimensional point measures of the vibroacoustic process can describe changes occurring as a result of the misfire very well. They may constitute the basis for the realization of the diagnostic procedure of misfire detection within on-board diagnostics – OBD II systems,
- the research at the potential operating conditions for a diesel locomotive engine confirmed a high precision and quality of the misfire detection (for each cylinder) with the help of the vibration acceleration. The obtained results proved a high precision of a diagnostic process for each engine cylinder,
- the JTFA method is characterized by a high dynamics of parameter changes, which reflects the occurrence or a lack of an ignition in an engine cylinder (34 dB for the 2112 SSF engine),
- the relative error of a method did not exceed 10% for the examined engines.

The tests on the 16H12A diesel locomotive engine gave the following conclusions:

- values of the dominant Lyapunov exponents were within the range 0.2–0.5. The increase in the dominant Lyapunov exponents was for the improper signals – by 17.9% on average, which indicates an increase in the misfire chaotic component – table 4.
- the most stable and univocal results were obtained for the engine speed of n = 1500 rpm (the average increase by 16.5%) and for 1100 rpm (the average increase by 4.6%).
- for 650 rpm the average increase was by 32.7%, but in this case the results were unstable and the t time-delay values differed for both proper and improper cases. It should also be remembered that in an idle run the operating conditions were very unstable.
- taking into consideration only the signals for 1100 and 1500 rpm, the measurements for three sensor directions were as follows:
  - for the direction horizontal–transverse to the main locomotive axis the average increase of the dominant Lyapunov exponent was 4.75%,
  - for the direction parallel to the main locomotive axis the average increase of the dominant Lyapunov exponent was 19.6%,
  - for the direction vertical–transverse to the main locomotive axis the average increase of dominant Lyapunov exponent was 7.4%.

Table 4

Relative increase in [%] of dominant Lyapunov exponents for the filtered signals obtained for the 16H12A engine

Type of case	An averaged increase [%]
All cases	17.9
For cylinder 1 inoperative	16.3
For cylinder 4 inoperative	19.5
For 1500 rpm	16.5
For 1100 rpm	4.6
For 650 rpm	32.7
Both for 1500 and 1100 rpm	10.6
Both for 1500 and 1100 rpm in direction Y	4.75
Both for 1500 and 1100 rpm in direction Z	19.6
Both for 1500 and 1100 rpm in direction X	7.4

The results of the research with the use of non-linear methods appear quite interesting. First of all, the dominant Lyapunov exponents for all signals were positive, which means that we can find some chaotic components in the signals and their dynamics. The calculated values of time delay τ and dimension d appeared quite reasonable. The d was moderately high which gives a hope to find some low-dimensional chaotic behavior. It is worth underlining that there exists a significant difference in the dominant Lyapunov exponents for the case with all cylinders working and the case with one cylinder disconnected. Taking into account the measurement presented in the paper and literature data we can conclude that the Lyapunov exponents can be used as diagnostic parameters. The only problem is to perform the good and reasonable reprocessing consisting of denoising and filtering. But the reprocessing should be performed with a great care because any inconsiderate elimination of some signal components can eliminate relevant dynamic information. Also some interesting behavior was observed during the use of the false nearest neighbor method. The result dimension of the method depends on the criterion threshold, which classifies neighbors as false or true. In the plot of dimension d against the criteria threshold we can find a broad plateau, which gives the possibility of a reasonable choice of the threshold and result dimension.

Nomenclature/*Skróty i oznaczenia*

a	Scale – a parameter connected with a placement in the frequency domain/*skala – parametr związany z położeniem w dziedzinie częstotliwości*
AFC	Amplitude-frequency correction/*korekcja-aplitudowo-częstotliwościowa*
AMI	Averaged mutual information/*uśredniona informacja wzajemna*
b	Parameter that points at a position in the time domain (translation)/*parametr określający położenie w dziedzinie czasu (translacja)*
CI	Compression-ignition/*zapłon samoczynny*
COR	Correlation function/*funkcja korelacji*
d	Dimension of the state space/*wymiar przestrzeni stanu*
D	Cylinder bore/*średnica cylindra* simple operation of the discrete Fourier transform/*prosta operacja dyskretnego przekształcenia Fouriera*
EOBD	European On-Board Diagnostics/*europejski system diagnostyki pokładowej*
ε	compression ratio/*stopień sprężania*
FFT	Fast Fourier Transform/*szybkie przekształcenie Fouriera*
FIR	Finite impulse response/*skończona odpowiedź impulsowa*
HDV	Heavy-Duty Vehicles/pojazdy ciężarowe o dopuszczalnej masie całkowitej powyżej 3500 kg
IIR	Infinite impulse response/*nieskończona odpowiedź impulsowa*
JTFA	Joint Time-Frequency Analysis/*analiza czasowo-częstotliwościowa*
λ	Lyapunov exponent/*wyikładnik Lapunowa*
M_o	Torque/moment obrotowy
n	Revolutions per minute/*prędkość obrotowa*
OBD	On-Board Diagnostics/diagnostyka pokładowa
OBD II	On-Board Diagnostics II (second generation)/*diagnostyka pokładowa drugiej generacji*
p_{wtr}	Injection opening pressure/*ciśnienie otwarcia wtryskiwacza*
S	Cylinder stroke/*skok tłoka*
s(t)	Sampled time signal run/wybrany przebieg czasowy sygnału
STFT	Short Time Fourier Transform/*krótkoczasowe przekształcenie Fouriera*
t	time, dynamic period/*czas, okres dynamiczny*
t_p	Sample time/*czas próbkowania*
τ	Position of the time window in the time domain, time delay in non-linear analysis/*położenie okna czasowego w dziedzinie czasu, opóźnienie czasowe w analizie nieliniowej*
V_{ss}	Engine displacement/*objętość skokowa silnika*
w(t)	Time window function (weighing function)/funkcja okna czasowego (funkcja wagowa)
WT	Wavelet Transform/przekształcenie falkowe
WVT	Wigner Ville Distribution/dystrybucja Wigner-Ville'a

Bibliography/*Literatura*

[1] Abarbanel H.D.I: Analysis of Observed Chaos Data. Springer 1996.

[2] Aittokallio T., Gyllenberg M., Hietarinta J., Kuusela T., Multama T.: Improving the false nearest neighbors method with graphical analysis, Physical Review 18 (1999) 416–421.

[3] Baker G. L., Gollub, J. P.: Wstęp do dynamiki układów chaotycznych. Wydawnictwo Naukowe PWN, Warszawa, 1998.

[4] Barczewski R., Szymański G. M.: Zastosowanie metod selekcji sygnału drganiowego w diagnostyce silników spalinowych. Pojazdy Szynowe 3–4/2004.

[5] Barczewski R., Tabaszewski M.: „Analiza przestrzenno-widmowa w diagnostyce złożonych obiektów mechanicznych". XXVI Ogólnopolskie Sympozjum „Diagnostyka Maszyn" Węgierska Górka 15–20.03.1999, Zeszyt 1/99.

[6] Barczewski R.: AFC – the method of amplitude spectrum correction. Congress of Technical Diagnostics, Gdańsk 1996.

[7] Barczewski R.: Analiza nieliniowości z zastosowaniem STSF-AFC jako metoda diagnozowania. II International Congress of Technical Diagnostics Warsaw, Poland 19–22 September 2000.

[8] Barczewski R.: Application of the Short Time Fourier Transform (STFT) with Amplitude and Frequency Correction (AFC) to non-linear system free vibration signal analysis. Report: CRI Hannover –DAAD, November 1997.

[9] Daily J. W.: Cycle-to-Cycle Variation: A Chaotic Processing?. Combustion Science and Technologies, 1988, Vol. 57, 149-162.
[10] Daw C. S., Kennel M. B., Finney C. E. A., Connolly F. T.: Observing and modelling nonlinear dynamics in an internal combustion engine. Physical Review E, Vol. 57, No. 3, 1998, 2811-2819.
[11] Foakes A. P., Pollard D. G.: Investigation of a Chaotic Mechanism for Cycle-to-cycle Variations. Combustion Science and Technology, 1993, Vol. 90, 281-287.
[12] Gorman M., El-Hamdi M., Robbins K. A.: Four Types of Chaotic Dynamics in Cellular Flames. Combustion Science and Technology, 1994, Vol. 98, 79-93.
[13] Iokibe T.: Industrial Application of Chaos Engineering. 2nd On-line Conference on Soft Computing in Engineering Design and Manufacturing (WSC2), 23-27 June 1997.
[14] Jerrelind J., Stensson A.: Nonlinear dynamics of parts in engineering systems. Chaos, Solitons and Fractals, 11, 2000, 2413-2428.
[15] Kantz H., Schreiber T.: Non-linear Time Series Analysis, Cambridge University Press, Cambridge, 1997.
[16] Kennel M. B., Brown R., Abarbanel H.D.I.: Determining embedding dimension for phase-space reconstruction using a geometrical construction, Physical Reviev A 45 (1992) 3403–3411.
[17] Li W., Gu F., Ball D., Leung A. Y. T, Phipps C. E.: A study of the noise from diesel engines using the independent component analysis. Mechanical Sytems and Signal Processing (2001) 15(6), pp. 1165-1184.
[18] Luo G., Xie J.: Bifurcations and chaos in a system with impacts. Physcia D, 148, 2001, 183-200.
[19] Marwala T., Hunt H. E. M.: Is damage identification using vibration data in a population of cylinders feasible? Journal of Sound and Vibration (2000) 237(4), pp. 727-732.
[20] Mitra, S.K., Kaiser J. F. (eds.): Handbook for Digital Signal Processing. John Wiley & Sons,1993.
[21] Newland D.E.: Practical Signal Analysis: Do Wavelets make any difference? Proceedings of DTC'97 1997 ASME Design Engineering Technical Conference, September 14-17, 1997 Sacramento, California.
[22] Ott E.: Chaos w układach dynamicznych. WNT, Warszawa, 1997.
[23] Rhodes C., Morari M.: False-nearest-neighbors algorithm and noise-corrupted time series, Physical Review E 55 (1997) 6162–6170.
[24] Roberts J. B., Peyton Jones J. C., Landsborough K. L.: Stochastical modelling and estimation for cyclic pressure variations in spark ignition engines. Mechanical Systems and Signal Processing (2001) 15(2), pp. 419-438.
[25] Shie Qian, Dapang Chen: Joint Time-Frequency analysis. Methods and Applications, Prentice Hall PTR Inc. 1996.
[26] Wang W. J, Chen J., Wu X. K., Wu Z. T.: The application of some non-linear methods in rotating machinery fault diagnosis. Mechanical Sytems and Signal processing (2001) 15(4), 697-705.
[27] Yang J., Pu L., Wang Z., Zhau Y., Yan X.: Fault detection in a Diesel engine by analysing the instantaneous angular speed. Mechanical Systems and Signal Processing (2001) 15(3), pp. 549-564.

Prof. Jerzy Merkisz, DSc., DEng. – Professor in the Faculty of Machines and Transport at Poznań University of Technology.

Prof. dr hab. inż. Jerzy Merkisz – profesor na Wydziale Maszyn Roboczych i Transportu Politechniki Poznańskiej.

Mr Marek Waligórski, DEng. – Doctor in the Faculty of Machines and Transport at Poznań University of Technology.

Dr inż. Marek Waligórski – adiunkt na Wydziale Maszyn Roboczych i Transportu Politechniki Poznańskiej.